In situ transport measurements on ultrathin Bi(111) films using a magnetic tip: possible detection of current-induced spin polarization in the surface states

2013 New J. Phys. 15 105018

(http://iopscience.iop.org/1367-2630/15/10/105018)

New Journal of Physics
The open access journal for physics

In situ transport measurements on ultrathin Bi(111) films using a magnetic tip: possible detection of current-induced spin polarization in the surface states

Takeshi Tono, Toru Hirahara[1] and Shuji Hasegawa
Department of Physics, University of Tokyo, 7-3-1 Hongo, Bunkyo-ku, Tokyo 113-0033, Japan
E-mail: hirahara@surface.phys.s.u-tokyo.ac.jp

New Journal of Physics **15** (2013) 105018 (14pp)
Received 27 May 2013
Published 21 October 2013
Online at http://www.njp.org/
doi:10.1088/1367-2630/15/10/105018

Abstract. We performed *in situ* transport measurements of ultrathin Bi(111) films grown on Si(111) surface, with a four-tip scanning tunneling microscope using metal-coated carbon nanotube (CNT) tips. When the distance between the current injection tip (nonmagnetic Pt-coated CNT tip) and voltage tip (magnetic CoFe-coated CNT tip) was smaller than 1 μm, we found a violation of Green's reciprocity theorem which should hold with no spin transport. This was interpreted as a signal of the current-induced spin polarization (CISP) that occurs due to the Rashba spin-splitting surface-state bands of the Bi(111). The result was reasonably in accord with quantitative analyses based on the CISP theory of Rashba systems.

[1] Author to whom any correspondence should be addressed.

Contents

1. Introduction 2
2. Experimental 4
3. Theory and measurement method 5
4. Results and discussion 8
5. Conclusion 13
Acknowledgments 13
References 13

1. Introduction

Spin-splitting in nonmagnetic materials has attracted much interest not only in terms of basic science but also for application to spintronic devices. The splitting becomes prominent when the space-inversion symmetry is broken for systems that have strong spin–orbit coupling. This was originally discussed for semiconductors with asymmetric structure such as the zinc blende structure (Dresselhaus effect), and extended to two-dimensional electron gases confined in asymmetric potentials (Rashba effect) [1]. Nowadays, the Rashba effect has been widely studied in surface systems [2] and even bulk polar semiconductors [3] with spin- and angle-resolved photoemission spectroscopy (ARPES).

Using these spin-split systems, we can expect spin-dependent transport just by applying an electric field or making electric current flow [4]. One of such phenomena is the spin Hall effect, in which a pure spin current flows transversely to the charge current. As a result, opposite spins accumulate at the opposite edges of the sample [5]. Another is called the current-induced spin polarization (CISP), in which spin polarization is induced in the flowing current. This can be understood in terms of the band structure. Figure 1(a) is the Fermi surface of an ideal Rashba spin-split free-electron system. The spin rotates clockwise (counterclockwise) for the inner (outer) Fermi ring with no out-of-plane components. Although there is local spin polarization in the momentum space, there remains no net spin polarization if we integrate all the spins at the whole Fermi surfaces. This is because there are opposite spins with the same wavenumber at the opposite side of the ring, resulting in cancelation with each other. This is consistent with the fact that the system is nonmagnetic.

However, when an electric field is applied in the $+x$ direction (the current is made flow in the $-x$ direction), the Fermi surface shifts as shown in figure 1(b). Now the center of the Fermi rings is at $(\delta k, 0)$, and as a result, the cancelation of the opposite spins at the opposite momentum is lost. For the electrons of the inner Fermi ring, the spins in the $-y$ direction become dominant, while the spins pointing in the $+y$ directions become dominant in the outer ring. Since the momentum for the electrons in the outer Fermi ring is larger than those for the inner one, a net spin polarization in the $+y$ direction is expected to remain in the current flowing in the $-x$ direction. This is the CISP phenomenon and should be observable using probes sensitive to spin polarization.

Such spin-dependent transport phenomena have been actually detected experimentally in semiconductor heterostructure systems [6, 7]. Compared to these systems, the Rashba surface states are known to host larger magnitude of the spin-spitting [8, 9] with complex Fermi surfaces, as shown in figure 1(c) for the Bi(111) surface as an example [9, 10]. It extends

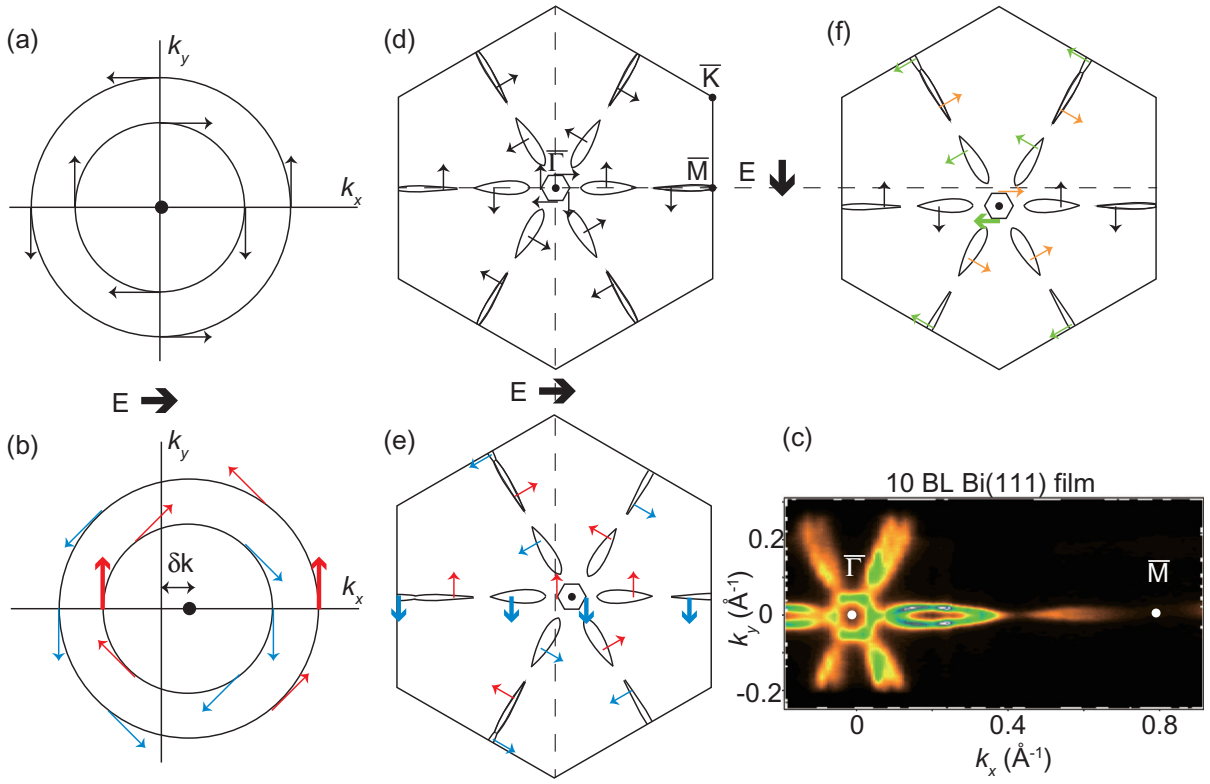

Figure 1. (a) Schematic drawing of the Fermi surface in an ideal Rashba spin-split free-electron system with the spin directions. By integrating the spin over the whole Fermi surface, there remains no net spin polarization. (b) By applying an electric field (E) in the x direction, the Fermi surface shifts by δk. Now there is a spin imbalance and a net spin polarization in the $+y$ direction. (c) The Fermi surface of a ten BL Bi(111) film measured by ARPES [10]. (d) Schematic drawing of the Fermi surface of Bi(111) in the surface Brillouin zone with the spin directions. Again, by integrating the spin over the whole Fermi surface, there is no net spin polarization. The z component of the spin [12, 13] has not been shown for clarity. (e) By applying an electric field (E) in the x ($\bar{\Gamma}$– $\bar{\mathrm{M}}$) direction, the Fermi surface shifts and a net spin polarization in the $-y$ ($\bar{\Gamma}$– $\bar{\mathrm{K}}$) direction is expected to appear. (f) By applying an electric field (E) in the $-y$ ($\bar{\Gamma}$– $\bar{\mathrm{K}}$) direction, the Fermi surface shifts and a net spin polarization in the $-x$ ($\bar{\Gamma}$– $\bar{\mathrm{M}}$) direction is expected to appear.

throughout the whole first surface Brillouin zone and is much larger than the bulk Fermi surface; the bulk Bi is a semi-metal while the surface is strongly metallic. Therefore, it has been shown that the surface-state conductivity is dominant for very thin Bi films [11]. Concerning the CISP, we now need to integrate the spins on the whole Fermi surfaces inside the first surface Brillouin zone under an electric field applied to see the spin imbalance. The magnitude of the induced spin polarization should be slightly different depending on the direction of the applied electric field, along the $\bar{\Gamma}$– $\bar{\mathrm{M}}$ or $\bar{\Gamma}$– $\bar{\mathrm{K}}$ directions (figures 1(e) and (f)) because the Fermi surface shape is different along the two directions. Furthermore, there are also out-of-plane components of spins which are omitted for clarity in figures 1(d)–(f) [12, 13]. Therefore the spin transport in

the Rashba surface systems should be intricate compared to the semiconductor heterostructures studied so far and maybe more promising for application. However, to our knowledge, there is no work reporting the spin-dependent transport phenomena in these systems. The main reason is that these surface states cannot survive in air and there have been no experimental apparatus that is capable of detecting spin-dependent transport *in situ* in ultrahigh vacuum (UHV).

In the present work, we have extended our nanometer-scale transport measurement technique in UHV [14–17] and performed *in situ* transport measurements of the surface states of ultrathin Bi(111) films with a four-tip scanning tunneling microscope (STM) using magnetic probes of CoFe-coated carbon nanotube (CNT) tips. We found that when the probe spacing is smaller than 1 μm, there was some signal of the detection of the CISP of the Rashba spin-split surface states. This was shown as a violation of Green's reciprocity theorem and was also supported by quantitative analyses. The present results opens a new field of surface-state spin transport and should stimulate further studies.

2. Experimental

The measurements were performed at room temperature (RT) in our four-tip STM system installed in an UHV scanning electron microscope (UHV SEM) [18]. Each probe can be independently driven with piezoelectric actuators and a scanner in *xyz* directions to achieve precise positioning in nanometer scales. The SEM was used for observing the tips for positioning, as well as the sample surface together with scanning reflection-high-energy electron diffraction capability. Its details are described elsewhere [18, 19]. The four-tip probes can be made contact with the sample surface in arbitrary arrangements, with marginal damage by a tunneling current approach and minute direct contact, which can be checked by SEM.

The metal-coated CNT tips were prepared by the following procedure. Firstly, multi-walled CNTs were sonicated in dichloroethane and attached at the apex of an electrochemically etched W wire by ac dielectrophoresis method [20]. The average diameter of the CNTs was about 20 nm. Secondly, the junction between the CNT and W supporting tip was reinforced by electron-beam induced deposition of hydrocarbon around the junction under SEM [21], followed by heating at 500 °C in high vacuum. Finally, the CNT-W tip was wholly coated with 10 nm thick Pt (nonmagnetic tips) or CoFe (magnetic tips) using the pulsed laser deposition technique [22]. This procedure is effective for stabilizing the resistance of the CNT-W junction down to less than 10 kΩ. Without the metal coating, the resistance at the CNT-W junction scattered from 100 kΩ to several MΩ from tip to tip, which was too high for the probes in conductivity measurements. The details of the tip fabrication and its electrical and mechanical characterizations are discussed elsewhere [23, 24].

After the tip preparation, they were taken out into air and transferred to the four-tip STM system. Platinum is known to be inert to oxidation, but CoFe should be a little oxidized during this transfer. The magnetization direction of the CoFe-coated CNT tip is in the axis direction of the CNT which is determined by the shape magnetic anisotropy; the aspect ratio of the CoFe film is 1:50–100. We have also applied a magnetic field as large as 150 mT along the CNT tip prior to installation, but the results did not seem to change whether the magnetic field was applied or not. This has also been demonstrated by magnetic force microscopy measurements for the CoFe-coated CNT tips with similar aspect ratio [25]. However since the tips are not

placed perpendicular to the surface but with an angle of 45° in our four-tip STM, these tips should be sensitive to both the in-plane and out-of-plane spin polarization.

For the sample preparation, a clean Si(111)-7 × 7 surface was prepared on an n-type substrate (P-doped, 1–10 Ω cm at RT) by a cycle of resistive heat treatments. Then Bi was deposited on the 7 × 7 surface at RT, followed by annealing at ∼ 380 K. Such procedure results in the formation of high-quality, single-crystalline, epitaxial Bi(111) films thicker than six BL (25 Å) as reported in [26, 27]. These films have a large surface-state Fermi surfaces (figure 1(c)) which show spin-splitting due to the Rashba effect [10, 28]. The thickness of the films in the present measurement was 10 BL, in which the surface-state contribution is over 60% of the total conductivity [11].

3. Theory and measurement method

In multiprobe conductivity measurements, it is often important to consider how many independent quantities there are by changing the measurement configuration. Usually, Green's reciprocity theorem is a relationship that holds for the charge (ρ) and the potential distribution (ϕ) that is determined by it as long as the time-reversal symmetry is not broken [29, 30]. Namely, it is expressed as

$$\int \rho\phi' \, \mathrm{d}V = \int \rho'\phi \, \mathrm{d}V, \tag{1}$$

where $\phi(\phi')$ is the electric potential resulting from a total charge density $\rho(\rho')$. From the Poisson's equation,

$$\nabla^2\phi = -\rho/\epsilon \tag{2}$$

holds, where ϵ is the permittivity of the material.

According to the Ohm's law (the current density is j, the electric field is E and the conductivity is σ)

$$\mathbf{j} = \sigma\mathbf{E} = -\sigma\nabla\phi. \tag{3}$$

Taking the divergence of the above, we obtain

$$\nabla^2\phi = -\nabla\cdot\mathbf{j}/\sigma. \tag{4}$$

Comparing this to equation (2), we can see that equation (4) is showing the Poisson's equation that defines the potential distribution that is made by current injectors ($\nabla\cdot\mathbf{j}/\sigma \to \rho/\epsilon$). From the above discussion, equation (1) can be rewritten as

$$\int (\nabla\cdot\mathbf{j})\phi' \, \mathrm{d}V = \int (\nabla\cdot\mathbf{j}')\phi \, \mathrm{d}V. \tag{5}$$

Now assume that multiple (n) point probes are attached to a conductor and the probe i is located at $\mathbf{r}_i$. Imagine a situation when each probe i injects current I_i and the potential distribution is initially ϕ. Then the divergence of the current density is given by

$$\nabla\cdot\mathbf{j} = \sum_{i=1}^{n} I_i\delta(\mathbf{r}-\mathbf{r}_i), \tag{6}$$

where δ is the Dirac delta function. When the injected current is changed to I_i', the potential distribution changes to ϕ'. According to Green's reciprocity theorem (equation (5)) and

equation (6),

$$\sum_{i=1}^{n} I_i \phi_i' = \sum_{i=1}^{n} I_i' \phi_i \tag{7}$$

should hold, where $\phi_i = \phi(\mathbf{r}_i)$ and $\phi_i' = \phi'(\mathbf{r}_i)$.

Now assume that multiple (n) probes are brought in contact with a conductor. We define the resistance $R_{ij;kl}$ as the measured resistance when the current is flown between probe k and l and the potential difference between probes i and j is measured, namely

$$R_{ij;kl} = \frac{\phi_i - \phi_j}{I_{k\to l}}. \tag{8}$$

In this case, the following three equations hold:

$$R_{ij;kl} = -R_{ij;lk} = -R_{ji;kl}, \tag{9}$$

$$R_{ij;kl} = R_{kl;ij}, \tag{10}$$

$$R_{ij;kl} + R_{ik;lj} + R_{il;jk} = 0. \tag{11}$$

Equation (9) is trivial (just by changing the polarity of the current or voltage measurements), so we will prove equations (10) and (11) below.

From the superposition principle,

$$\phi_i = \sum_{i=1}^{n} R_{ij} I_j \tag{12}$$

should hold, where R_{ij} is the resistance (including the sign) between probes i and j. Combining equations (7) and (12), we obtain $R_{ij} = R_{ji}$. Using this,

$$R_{ij;kl} = \frac{\phi_i - \phi_j}{I_{k\to l}} = R_{ik} - R_{il} - R_{jk} + R_{jl} \tag{13}$$

can be obtained using $I_k = -I_l = I_{k\to l}$, $I_m = 0$ for $m \neq k, l$. Similarly,

$$R_{kl;ij} = R_{ki} - R_{kj} - R_{li} + R_{lj} \tag{14}$$

and equation (10) can be obtained using $R_{ij} = R_{ji}$. Furthermore, equation (11) can be obtained from the three equations below:

$$R_{ij;kl} = R_{ik} - R_{il} - R_{jk} + R_{jl}, \tag{15}$$

$$R_{ik;lj} = R_{il} - R_{ij} - R_{kl} + R_{kj}, \tag{16}$$

$$R_{il;jk} = R_{ij} - R_{ik} - R_{lj} + R_{lk}. \tag{17}$$

Using both equations (10) and (11),

$$R_{kl;ij} + R_{lj;ik} + R_{jk;il} = 0 \tag{18}$$

holds. This is true as long as time-reversal symmetry is conserved, i.e. as long as there is no magnetic field applied or no magnetic materials/signals are involved. Therefore, we can say that independent values of resistance in the four-point probe measurement are only two of the six possible values; the resistance values obtained with any other combinations of probes are derived from the two values using the relations above.

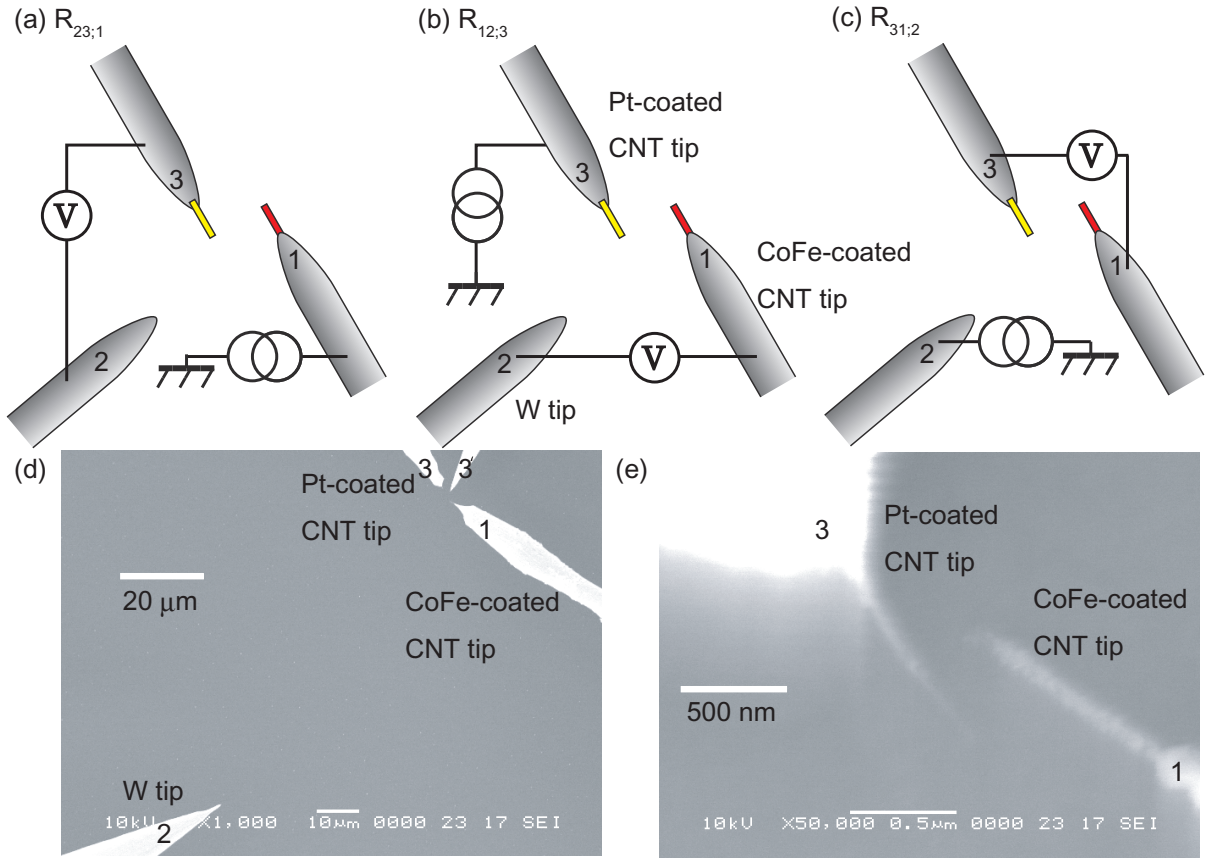

Figure 2. (a)–(c) Schematic drawing of the three configurations of the current–voltage (I–V) measurements using the W, Pt-coated CNT and CoFe-coated CNT tips. According to Green's reciprocity theorem, $R_{23;1} + R_{12;3} + R_{31;2} = 0$ should hold. (d), (e) SEM images of the actual probe arrangement on Bi(111) surface. Panel (e) is an enlarged image of (d) to recognize the CNT tips.

In our measurements, we basically use three tips and the sample itself as the fourth probe and always flow the current from one of the probes to the sample. Therefore, we will write $R_{ij;k}$ as the measured resistance when the current is flown between probe k and the sample and the potential difference between probes i and j is measured where $\{i, j, k\}$=$\{1, 2, 3\}$. There are three different configurations as shown in figures 2(a)–(c) and according to equation (18), they are related as

$$R_{23;1} + R_{12;3} + R_{31;2} = 0 \tag{19}$$

as long as the time-reversal symmetry is conserved. Reversely, in order to obtain a signal related to the spin dependent transport, we should check whether this relation is violated or not.

We have used a CoFe-coated CNT tip as one of the probes. Since a magnetic probe and a nonmagnetic one should measure a different voltage drop (ΔV) if there is spin polarization in the measured sample, the observation of a nonzero sum of equation (19) using a magnetic probe should imply the detection of a spin signal. To say it more quantitatively, ΔV can be written

as [31]

$$\Delta V = \eta \left| \frac{\mu_\uparrow - \mu_\downarrow}{2} \right| \mathbf{m} \cdot \mathbf{s}, \tag{20}$$

where $|\frac{\mu_\uparrow - \mu_\downarrow}{2}|$ is the difference of the chemical potential of the magnetized sample and $\mathbf{m} \cdot \mathbf{s}$ corresponds to the normalized inner product of the tip magnetization and the sample spin polarization. η is the efficiency of the magnetic probes which is determined by the conductivity of the majority and minority spins (0.65 in our CoFe film [32]). Considering the fact that the probes are inclined by 45° with respect to the surface normal in our four-tip STM, this reduces to $0.65 \times \sin 45^\circ \sim 0.5$ in our measurements.

In summary, the idea of our measurement to measure the CISP of the Bi surface state is to measure the nonzero value of

$$\Delta R = R_{23;1} + R_{12;3} + R_{31;2} \tag{21}$$

using a CoFe-coated CNT tip. ΔR should be zero as long as we are using only nonmagnetic tips that cannot detect the spin signal. Figures 2(d) and (e) show the actual SEM images of the probes we have used. One of the tips is just the usual W tip (tip 2). Two others are Pt-coated CNT tips (nonmagnetic probes, 3 and 3′) and the last one is the CoFe-coated CNT tip (tip 1). We basically fix the tips 1 and 2 and shifted the tip 3 for measuring the probe spacing dependence. The reason why there are two probes for tip 3 is that their individual movement is limited and the two are complementary to obtain the whole data set.

4. Results and discussion

As described in the previous section, we have changed the combinations of the probes for current injection and potential drop measurements (figures 2(a)–(c)), and tried to deduce the spin transport signal as a violation of Green's reciprocity theorem. Figures 3(b)–(d) show the measured values of $R_{23;1}$, $-R_{12;3}$ and $R_{31;2}$, respectively, as a function of the distance d of the CoFe- (tip 1) and Pt-coated (tip 3) CNT tips (see figure 3(a) for the definition of d). The measured values $R_{23;1}$ and $-R_{12;3}$ are shown in logarithmic scale of d. The different colors of the data points in figures 3(b)–(d) show the different relative positions between the tips 1 and 3 as shown in figure 3(a). The data points in figures 3(b) and (c) can be fitted to the probe spacing dependence of the resistance of a two-dimensional conductor (neglecting the contribution from the spin-dependent potential)

$$R = -\frac{1}{2\pi\sigma_{2D}} \log \frac{d}{d_{\mathrm{effCoFe-W}}} \tag{22}$$

with σ_{2D} and $d_{\mathrm{effCoFe-W}}$ as the fitting parameters, where σ_{2D} is the two-dimensional conductivity and $d_{\mathrm{effCoFe-W}}$ is the distance between the CoFe-coated CNT (tip 1) and W (tip 2) probes. The fitted curve is shown in figures 3(b) and (c) which give $\sigma_{2D} = 3.3\,\mathrm{mS}$ and $d_{\mathrm{effCoFe-W}} \sim 100\,\mu\mathrm{m}$. The obtained σ_{2D} is slightly larger than that obtained in a previous report of Bi(111) surface (2.2 mS [11]) and $d_{\mathrm{effCoFe-W}}$ is nearly the same as the set value of 90 μm in figure 2(a). For the data of figure 3(d), the probe spacing between the voltage probes (tips 1 and 3) was so small compared to the distance between the current injection probe (tip 2) and those voltage probes that we could not obtain a reliable fitting, although it can be seen to some extent that the absolute value of the measured resistance does increase by increasing the probe spacing.

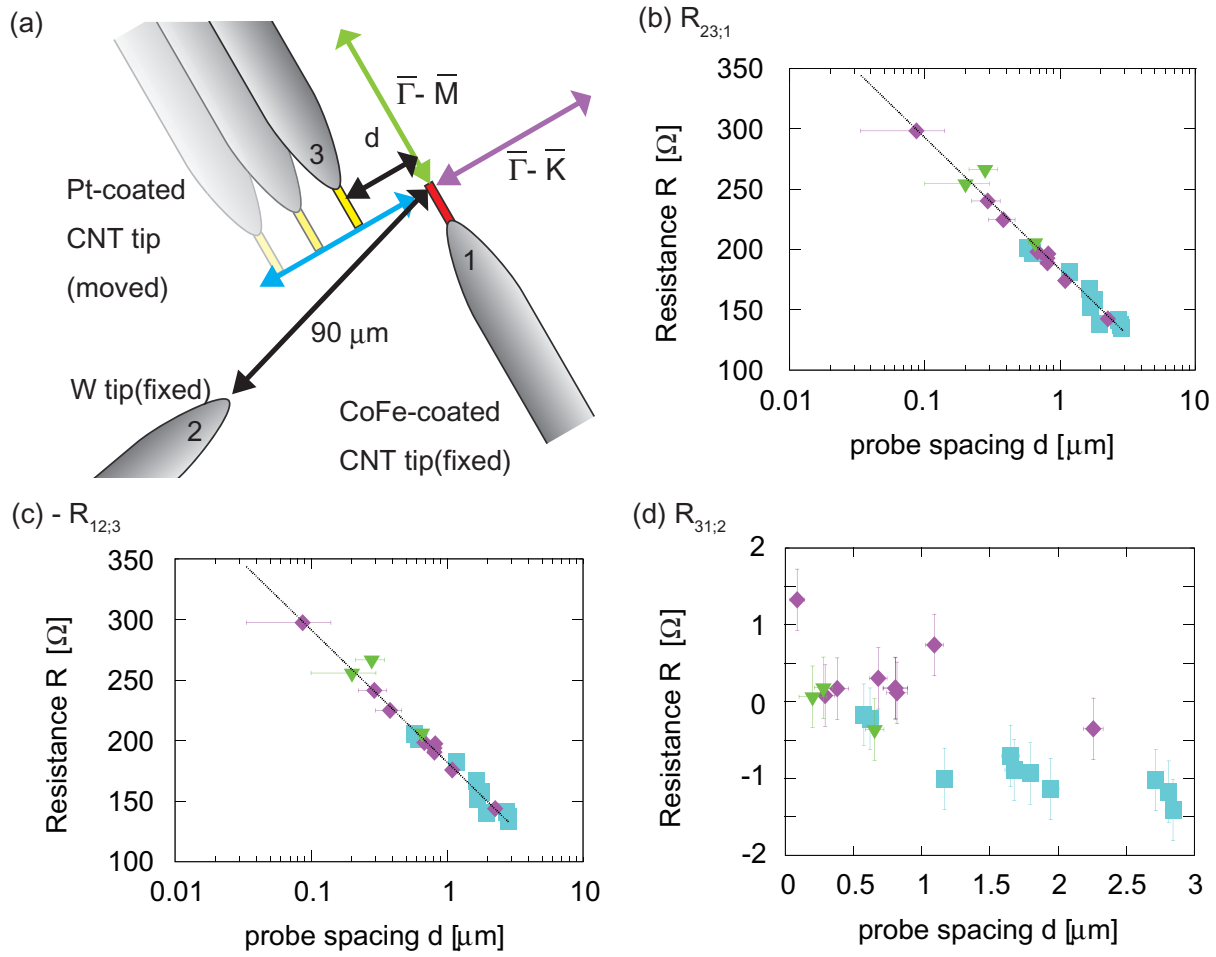

Figure 3. Schematic drawing of the measurements using the W, Pt-coated CNT and CoFe-coated CNT tips. (b)–(d) The actual results of $R_{23;1}$ (b), $-R_{12;3}$ (c), $R_{31;2}$ (d), respectively, measured for Bi(111) surface at RT. Green, light blue and purple corresponds to the relative position of tips 1 and 3 in (a). The dashed lines in show the results of the fitting to equation (22).

Now let us discuss if Green's reciprocity theorem still holds in our measurements or not. Figure 4(a) shows the $\Delta R = R_{23;1} + R_{12;3} + R_{31;2}$ as a function of the probe position x (see figure 4(d)) calculated from the data sets in Fig 3. ($x = d$ when the tip 3 is placed on the right side of the tip 1 (purple data points), while $x = -d$ when the tip 3 is on the left side of the tip 2 (light blue data points).) We can see that ΔR deviates from zero, with opposite signs depending on the relative position of the probes, in the range of $|x| \leqslant 1\ \mu$m for the data points of light blue and purple which are data along the $\bar{\Gamma}$– $\bar{\mathrm{K}}$ direction. However, the data points by shifting the probe along $\bar{\Gamma}$– $\bar{\mathrm{M}}$ direction (shown by green points) are nearly zero even when $|x| \leqslant 1\ \mu$m. To check if the nonzero signal is really related to the detection of spin-dependent potential using the CoFe-coated CNT tip, we did the same measurement with nonmagnetic tips only; tip 1 was replaced with a Pt-coated CNT tip. The result is shown in figure 4(b) and ΔR is nearly zero for the whole range of d, even when the probe spacing is smaller than 1 μm. Therefore it is highly possible that we are detecting some spin-dependent transport signal in figure 4(a).

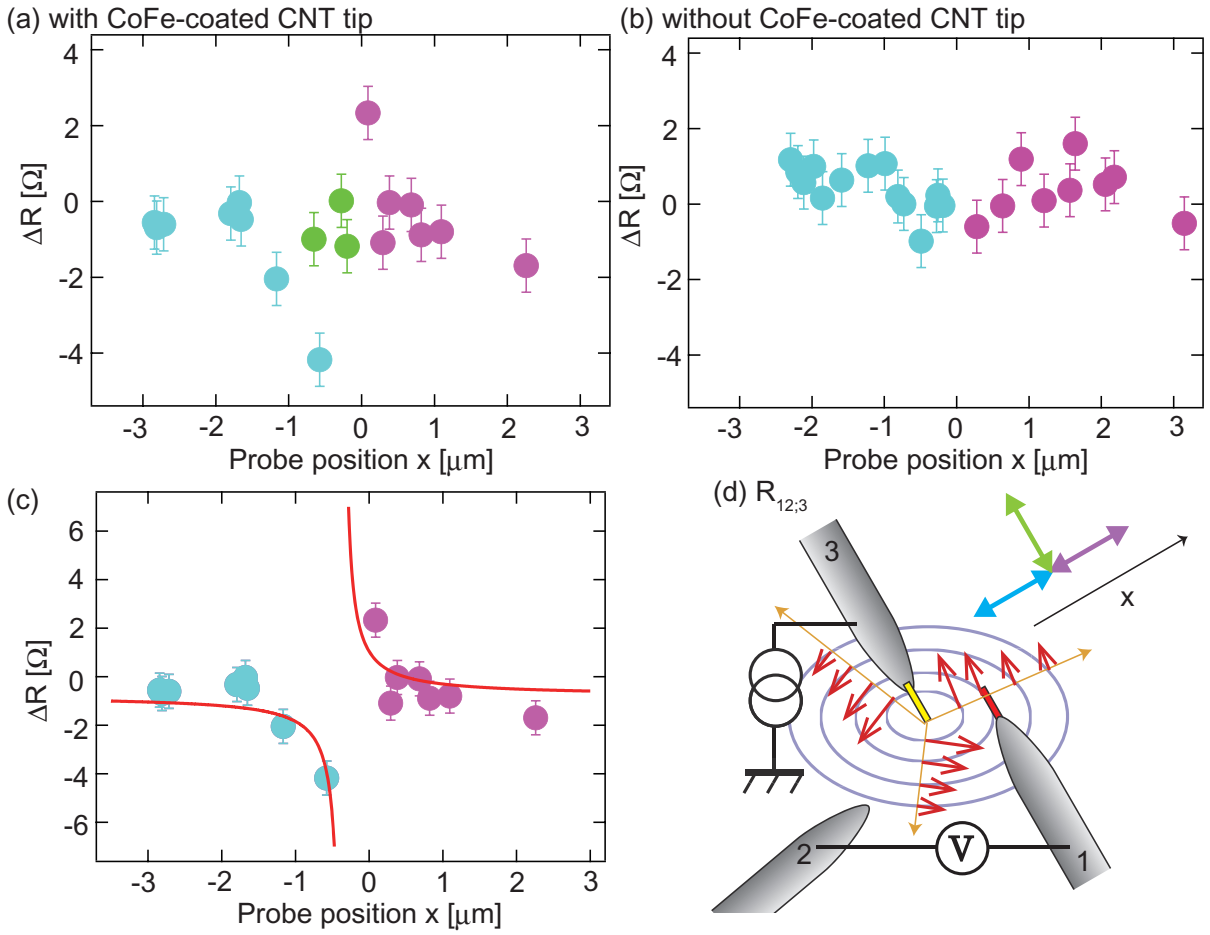

Figure 4. (a) The sum $\Delta R = R_{23;1} + R_{12;3} + R_{31;2}$ from the data of figure 3. (b) Same as (a) but when the CoFe-coated CNT magnetic tip was replaced with a nonmagnetic Pt-coated CNT tip. ΔR is nearly zero for all the data points in (b) while it shows deviation from zero for the light blue and purple points near $x = 0$ in (a). (c) The results of (a) replotted together with the fitting curve of equation (29). (d) Schematic drawing of the present CISP measurement. The spin-dependent potential induced by the current injection from the Pt-coated CNT tip (3) into the sample is measured by the CoFe-coated CNT tip (1). The orange arrow shows the current flow, the blue concentric circles show the equi-potential lines, and the red arrows show the induced spin polarization.

What kind of spin signal is actually detected in figure 4(a)? Let us now examine some possibilities based on the configurations shown in figures 2(a)–(c). In figure 2(a), the current is injected from the CoFe-coated CNT tip into the sample. This means the injection of a spin-polarized current. Since in the Rashba system the spin is locked to the momentum (figure 1), such spin-polarized carrier should flow along a particular direction and can results in a direction-dependent chemical potential. But such spin can precess (relax) while flowing. If the distance between the injector (tip 1) and detector (tip 3) is larger than the spin relaxation length, there should be no effect of the spin-polarized carriers. Since the minimum spacing of the probes is

$\sim$100 nm which should be larger than the spin relaxation length on Bi(111) at RT, we believe that it is not realistic that we have detected such a signal[2].

Next let us consider the situation in figure 2(b) in which the current is injected from the nonmagnetic tip (tip 3) into the sample and the magnetic tip (tip 1) is used in the potential measurement. The current should flow out isotropically way around the tips 3 as shown by orange arrows in figure 4(d), and due to the spin orientation locked with the momentum, the induced spin should be perpendicular to the current direction and rotating as shown by red arrows in the figure. Therefore depending on the relative direction between the magnetization of tip 1 and the induced spin in the current, we should be able to observe spin-dependent voltages because of a difference between the spin-dependent chemical potentials $\mu_\uparrow$ and $\mu_\downarrow$ (see equation (21)). However, the magnitude of the spin polarization should decrease as the distance between the tips 1 and 3 becomes larger since the current density is decreasing. This should make the observed signal smaller. These characteristics seem to be consistent with what we have observed in figure 4(a) where the signal becomes almost zero at larger distances. In the $+x$ direction (purple) in figure 4(d), the tip magnetization and CISP direction are parallel with each other, while for the $-x$ (light blue) direction, they are antiparallel. This leads to the positive and negative ΔR in figure 4(a), respectively, by considering equation (20). For the direction indicated by green, the tip magnetization and the CISP direction are nearly perpendicular to each other and hence always $\Delta V = 0$ ($\Delta R = 0$) irrespective of the distance between the tips 1 and 3. The same picture can basically be applied to the measurement of figure 2(c). But the distance between the current injector (tip 2) and the spin-sensitive detector (tip 3) is so far away (90 μm) that the current density is small to induce a noticeable spin-polarization signal. Therefore, we can say that the violation of Green's reciprocity theorem (nonzero value of ΔR) comes from $R_{12;3}$ mainly[3].

Our consideration above is further corroborated by the quantitative analyses. According to [35], the expectation value of the induced spin-polarization in a Rashba system can be written as

$$\mathbf{s} = -\frac{\hbar}{2} \tanh \frac{\Delta_k}{k_\mathrm{B} T} \hat{\mathbf{B}}_\mathrm{eff}, \tag{23}$$

where $\Delta_k = \alpha_\mathrm{R} \delta k$ is the energy splitting between the two spin orientations at the Fermi level which is determined by the Rashba parameter α_R and the shift of the Fermi surface $\delta \mathbf{k} = \frac{e\tau}{\hbar}\mathbf{E}$ under the electric field $\mathbf{E}$ applied (τ is the momentum relaxation time). $\hat{\mathbf{B}}_\mathrm{eff}$ is the unit vector of the direction of the effective magnetic field due to the Rashba effect. In our case, the above

[2] There are no experimental reports on the spin relaxation length of Bi. However, since Bi is a heavy atom showing strong spin–orbit coupling effects, the spin relaxation length should not be so long. In fact heavy atoms such as Pt, Pd or Au all show a spin diffusion length about several to several ten nm at room temperature [33, 34]. Furthermore, in the Bi surface states, the Rashba effect should be another source for the spin relaxation. Therefore, it is likely that the spin diffusion length of the Bi(111) surface states at room temperature should be less than 100 nm.

[3] One may worry about the influence of the stray magnetic field of these tips. In [25], it is shown that the stray field of these CNT tips are much smaller than the conventional magnetic metal probes used in magnetic force microscopy measurements. Furthermore, the Hall effect due to the stray field cannot be the origin of the sign change of the data points of light blue and purple shown in figure 4(a) since they should be symmetric with respect to the plane which includes the magnetic tip and normal to the surface. Such a signal, if it exists, should give identical contributions (same sign) in both directions, which is clearly in contradiction to the data shown in figure 4(a).

equation should be rewritten as

$$\mathbf{s} \simeq -\frac{\hbar}{2}\frac{\alpha_{\mathrm{R}}}{k_{\mathrm{B}}T}\frac{\mathrm{e}\tau}{\hbar}|\mathbf{E}|\hat{\boldsymbol{\theta}}, \tag{24}$$

since the induced spin polarization is very small and the effective magnetic field is parallel to the tangential direction $\hat{\boldsymbol{\theta}}$.[4] The spin density s_{D} which is the measured physical quantity is related to $\mathbf{s}$ by

$$s_{\mathrm{D}} = eN_0\left|\frac{\mu_\uparrow - \mu_\downarrow}{2}\right| = \frac{|\mathbf{s}|}{A}\frac{2}{\hbar}, \tag{25}$$

where N_0 is the density of state at the Fermi level and A is the area of the unit cell of the surface crystal lattice. Therefore, the chemical potential difference due to the CISP is expressed as

$$\left|\frac{\mu_\uparrow - \mu_\downarrow}{2}\right| = \frac{1}{AN_0}\frac{\alpha_{\mathrm{R}}}{k_{\mathrm{B}}T}\frac{\tau}{\hbar}|\mathbf{E}|. \tag{26}$$

Since, due to the two-dimensionality of the system, the electric field induced by the current in the present measurement is expressed as

$$\mathbf{E} = \frac{I}{2\pi\sigma_{2\mathrm{D}}r}\hat{\mathbf{r}}, \tag{27}$$

where $\hat{\mathbf{r}}$ is the unit vector along the radial direction, equation (26) can be rewritten as

$$\left|\frac{\mu_\uparrow - \mu_\downarrow}{2}\right| = \frac{1}{AN_0}\frac{\alpha_{\mathrm{R}}}{k_{\mathrm{B}}T}\frac{\tau}{\hbar}\frac{I}{2\pi\sigma_{2\mathrm{D}}r}. \tag{28}$$

Finally, the measured ΔR can be expressed as

$$\Delta R = \eta\frac{\mu_\uparrow - \mu_\downarrow}{2}/I = \frac{\eta}{AN_0}\frac{\alpha_{\mathrm{R}}}{k_{\mathrm{B}}T}\frac{\tau}{\hbar}\frac{1}{2\pi\sigma_{2\mathrm{D}}x}. \tag{29}$$

The solid lines in figure 4(c) shows the fitted results to equation (29) (the origin has been slightly shifted to compensate for the uncertainty in the actual probe contact position and the position of $\Delta R = 0$). Using $N_0 \sim 10^{14}\,\mathrm{eV}^{-1}\,\mathrm{cm}^{-2}$, $\alpha_{\mathrm{R}} \sim 0.73\,\mathrm{eV\,\AA}$, $A = \sqrt{3} \times 4.54^2/2\,\mathrm{\AA}^2$, $T = 300\,\mathrm{K}$, $\sigma_{2\mathrm{D}} = 3.3\,\mathrm{mS}$ and $\eta \sim 0.5$, we obtain the momentum relaxation time $\tau \sim 10^{-15}\,\mathrm{s}$. This is in the same order of magnitude as other surface states at RT [14, 36]. This value is also consistent with the lifetime of the Bi(111) surface states determined from ARPES analysis [37]. These facts suggest that our analysis based on the surface-state CISP is plausible.

From the above fitting, we can deduce the difference between the spin-dependent chemical potentials $\frac{\mu_\uparrow - \mu_\downarrow}{2}$ and the spin density s_{D}, both of which depend on the probe spacing r (equation (28)). They are summarized in table 1. There is several tens to several hundreds μV of potential difference when r is smaller than 1 μm which decays quickly with r, making the detection of the CISP signal impossible for $r > 1\,\mu$m.

Our results show that there is some spin-dependent transport phenomenon occurring at the surface of Bi(111), a Rashba spin-split system, which is likely the CISP. One drawback of the present measurement is that we are not able to change the magnetization direction of the tip at will *in situ*. There is no apparatus to apply a magnetic field in our four-tip STM, and

[4] We neglect the out-of-plane spin component [12, 13] for the sake of simplicity.

Table 1. The difference of the spin-dependent chemical potential $\frac{\mu_\uparrow - \mu_\downarrow}{2}$ and the induced spin density s_D in the current, obtained by the fitting in figure 4(c).

Probe spacing (nm)	$\frac{\mu_\uparrow - \mu_\downarrow}{2}$ (μV)	s_D (μm^{-2})
10	300	800
100	30	80
1000	3	8

furthermore, the CNT tips are broken easily after some measurements. Further sophisticated studies that combines the ability to cool down the sample and the tip, and to apply a magnetic field to change the tip magnetization as well as an easy handling method of the CNT tips are needed for the detailed analysis of the surface-state CISP. Especially, if we can make the current path with a narrow wire structure on Bi(111) surface, we will be able to detect a larger CISP signal, because the current density, and therefore, the induced spin density do not decrease with the tip distance. We are now preparing such samples with *in situ* micro-fabrication techniques.

5. Conclusion

In summary, we have performed *in situ* transport measurements of ultrathin Bi(111) films with a four-tip STM using a magnetic probe of a CoFe-coated CNT tip. When the probe spacing between the current source and voltage measurement was smaller than 1 μm, we were able to detect a signal of the detection of the CISP of the Rashba spin-split surface states. This was also supported by quantitative analyses based on the CISP theory of Rashba effect. Further elaborated studies are needed to unveil the peculiar spin-dependent transport properties in these systems.

Acknowledgments

This work was supported by Grants-In-Aid from Japan Society for the Promotion of Science (numbers 22656011 and 23686007).

References

[1] Winkler R 2003 *Spin–Orbit Coupling Effects in Two-Dimensional Electron and Hole Systems* (Berlin: Springer)
[2] Dil J H 2009 *J. Phys.: Condens. Matter* **21** 403001
[3] Ishizaka K *et al* 2011 *Nature Mater.* **10** 521
[4] Awschalom D and Samarth N 2009 *Physics* **2** 50
[5] Kato Y K, Myers R C, Gossard A C and Awschalom D D 2010 *Science* **306** 1910
[6] Sih V, Myers R C, Kato Y K, Lau W H, Gossard A C and Awschalom D D 2005 *Nature Phys.* **1** 31
[7] Brüne C, Roth A, Novik E G, König M, Buhmann H, Hankiewicz E M, Hanke W, Sinova J and Molenkamp L W 2010 *Nature Phys.* **6** 448
[8] Ast C, Henk J, Ernst A, Moreschini L, Falub M, Pacilé D, Bruno P, Kern K and Grioni M 2007 *Phys. Rev. Lett.* **98** 186807

[9] Koroteev Y M, Bihlmayer G, Gayone J E, Chulkov E V, Blügel S, Echenique P M and Hofmann P 2004 *Phys. Rev. Lett.* **93** 046403
[10] Hirahara T, Nagao T, Matsuda I, Bihlmayer G, Chulkov E V, Koroteev Y, Echenique P M, Saito M and Hasegawa S 2006 *Phys. Rev. Lett.* **97** 146803
[11] Hirahara T, Matsuda I, Yamazaki S, Miyata N, Hasegawa S and Nagao T 2007 *Appl. Phys. Lett.* **91** 202106
[12] Takayama A, Sato T, Souma S and Takahashi T 2011 *Phys. Rev. Lett.* **106** 166401
[13] Miyahara H, Maegawa T, Kuroda K, Kimura A, Miyamoto K, Namatame H, Taniguchi M and Okuda T 2012 *e-J. Surf. Sci. Nanotechnol.* **10** 153
[14] Kanagawa T, Hobara R, Matsuda I, Tanikawa T, Natori A and Hasegawa S 2003 *Phys. Rev. Lett.* **91** 036805
[15] Tanikawa T, Matsuda I, Kanagawa T and Hasegawa S 2004 *Phys. Rev. Lett.* **93** 016801
[16] Yamada M, Hirahara T and Hasegawa S 2013 *Phys. Rev. Lett.* **110** 237001
[17] Yoshimoto S *et al* 2007 *Nano Lett.* **7** 956
[18] Shiraki I, Tanabe F, Hobara R, Nagao T and Hasegawa S 2001 *Surf. Sci.* **493** 633
Hasegawa S, Shiraki I, Tanabe F and Hobara R 2002 *Curr. Appl. Phys.* **2** 465
[19] Shiraki I, Nagao T, Hasegawa S, Petersen C L, Boggild P, Hansen T M and Grey F 2000 *Surf. Rev. Lett.* **7** 533
[20] Tang J, Gao B, Geng H, Velev O D, Qin L C and Zhou O 2003 *Adv. Mater.* **15** 1352
[21] Koops H W P, Kretz J, Rudolph M, Weber M, Dahm G and Lee K L 1994 *Japan. J. Appl. Phys.* **33** 7099
[22] Ikuno T, Katayama M, Kamada K, Honda S, Lee J G, Mori H and Oura K 2003 *Japan. J. Appl. Phys.* **42** L1356
Ikuno T, Yasuda T, Honda S, Oura K, Katayama M, Lee J G and Mori H 2005 *J. Appl. Phys.* **98** 114305
[23] Yoshimoto S *et al* 2005 *Japan. J. Appl. Phys.* **44** L1563
[24] Konishi H *et al* 2006 *Japan. J. Appl. Phys.* **45** 3690
[25] Kuramochi H, Uzumaki T, Yasutake M, Tanaka A, Akinaga H and Yokoyama H 2005 *Nanotechnology* **16** 24
Kuramochi H, Manago T, Koltsov D, Takenaka M, Iitake M and Akinaga H 2007 *Surf. Sci.* **601** 5289
[26] Nagao T, Sadowski J, Saito M, Yaginuma S, Fujikawa Y, Kogure T, Ohno T, Hasegawa Y, Hasegawa S and Sakurai T 2004 *Phys. Rev. Lett.* **93** 105501
[27] Yaginuma S, Nagao T, Sadowski J T, Pucci A, Fujikawa Y and Sakurai T 2003 *Surf. Sci.* **547** L877
[28] Hirahara T *et al* 2008 *New J. Phys.* **10** 083038
[29] Jackson J D 1998 *Classical Electrodynamics* 3rd edn (New York: Wiley)
[30] Büttiker M 1986 *Phys. Rev. Lett.* **57** 1761
[31] Zhang S 2000 *Phys. Rev. Lett.* **85** 393
[32] Bass J and Pratt W P Jr 1999 *J. Magn. Magn. Mater.* **200** 274
[33] Niimi Y, Wei D, Idzuchi H, Wakamura T, Kato T and Otani Y 2012 *Phys. Rev. Lett.* **110** 016805
[34] Vlaminck V, Pearson J E, Bader S D and Hoffmann A 2013 *Phys. Rev.* B **88** 064414
[35] Liu M H, Chen S H and Chang C R 2008 *Phys. Rev.* B **78** 165316
[36] Matsuda I and Hasegawa S 2007 *J. Phys.: Condens. Matter* **19** 355007
[37] Gayone J E, Kirkegaard C, Wells J W, Hoffmann S V, Li Z and Hofmann P 2005 *Appl. Phys.* A **80** 943